

---

# Disentangling Improves VAEs' Robustness to Adversarial Attacks

---

Matthew Willetts\*, Alexander Camuto\*, Stephen Roberts, Chris Holmes  
University of Oxford  
Alan Turing Institute  
{mwilletts, acamuto, sroberts, cholmes}@turing.ac.uk

## Abstract

This paper is concerned with the robustness of VAEs to adversarial attacks. We highlight that conventional VAEs are brittle under attack but that methods recently introduced for disentanglement such as  $\beta$ -TCVAE (Chen et al., 2018) improve robustness, as demonstrated through a variety of previously proposed adversarial attacks (Tabacof et al. (2016); Gondim-Ribeiro et al. (2018); Kos et al.(2018)). This motivated us to develop *Seatbelt-VAE*, a new hierarchical disentangled VAE that is designed to be significantly more robust to adversarial attacks than existing approaches, while retaining high quality reconstructions.

## 1 Introduction

Unsupervised learning of disentangled latent variables in generative models remains an open research problem, as is an exact mathematical definition of disentangling [1]. Intuitively, a disentangled generative model has a one-to-one correspondence between each input dimension of the generator and some interpretable aspect of the data generated.

For VAE-derived models [2, 3] this is often based around rewarding independence between latent variables. Factor VAE [4],  $\beta$ -TCVAE [5] and HFVAE [6] have shown that the evidence lower bound can be decomposed to obtain a term capturing the degree of independence between latent variables of the model, the total correlation. By up-weighting this term, we can obtain better disentangled representations under various metrics compared to  $\beta$ -VAEs [7].

Disentangled representations, much like PCA or Factor analysis, are not only human-interpretable but also offer more informative and robust latent space representations. In addition, information theoretic interpretations of deep learning show that having a disentangled hidden layer within a discriminative deep learning model increases robustness to adversarial attack [8].

Adversarial attacks on deep generative models, more difficult than those on discriminative models [9, 10, 11], attempt to fool a model into reconstructing a chosen target image by adding distortions to the original input image. Generally, the most effective attack mode involves making the latent-space representation of the distorted input match that of the target image [10, 11]. This kind of attack is particularly relevant to applications where the encoder's output is used downstream.

Projections of data from VAEs, disentangled or not, are used for tasks such as: text classification [12]; discrete optimisation [13]; image compression [14, 15]; and as the perceptual part of a reinforcement learning algorithm [16, 17], the latter of which uses a disentangled VAE's encoder to improve the robustness of the agent to domain shift.

Here we demonstrate that  $\beta$ -TCVAEs are significantly more robust to 'latent-space' attack than standard VAEs, and are generally more robust to attacks that act to maximise the evidence lower

---

\* Willetts and Camuto contributed equally to this work.

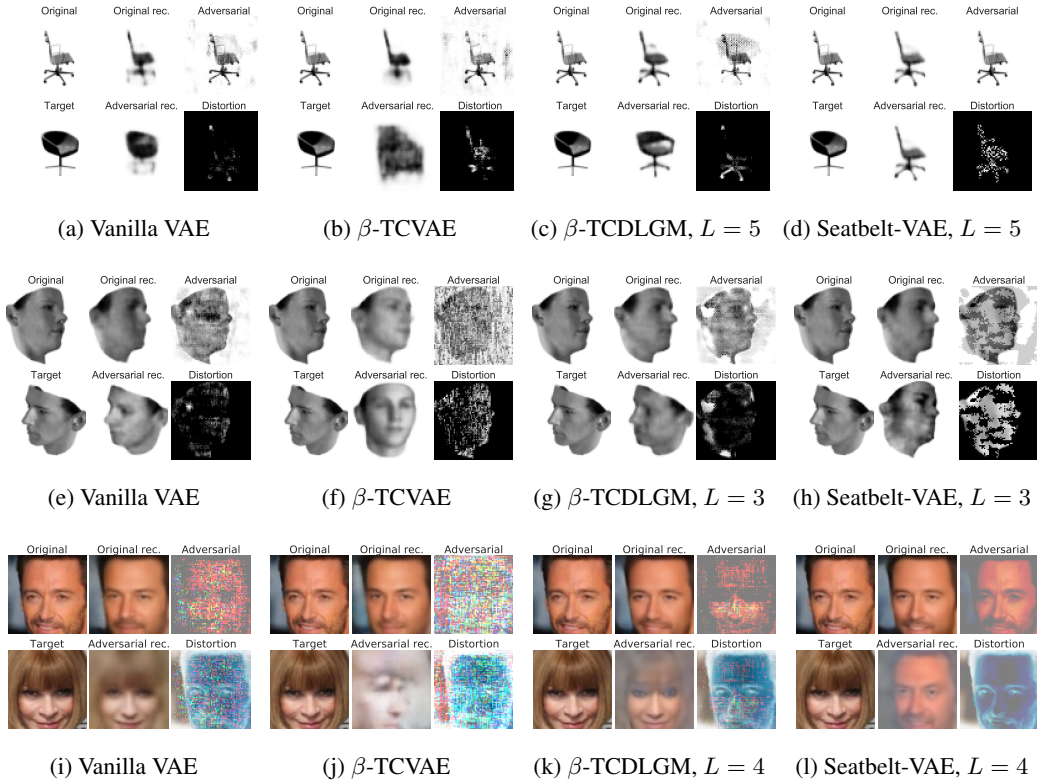


Figure 1: Latent-space adversarial attacks on Chairs, 3D Faces and CelebA for different models, including our proposed *Seatbelt-VAE*.  $\beta = 10$  for  $\beta$ -TCVAE,  $\beta$ -TCDLGM and *Seatbelt-VAE*.  $L$  is the number of stochastic layers. Clockwise within each plot we show the initial input, its reconstruction, the adversarial input, the adversarial distortion added to make it (shown normalised), the adversarial input’s reconstruction, and the target image.

bound for the adversarial input. The robustness of these disentangled models is highly relevant because of the use-cases for VAEs highlighted above.

However, imposing additional disentangling constraints on a VAE training objective degrades the quality of resulting drawn or reconstructed images [7, 5]. We sought whether more powerful, expressive models, can help ameliorate this and in doing so built a hierarchical disentangled VAE, *Seatbelt-VAE*, drawing on works like Ladder VAEs [18] and BIVA [19]. *Seatbelt-VAEs* are more robust to adversarial attacks than  $\beta$ -TCVAEs and  $\beta$ -TCDLGMs (the latter a simple generalisation we make of  $\beta$ -TC penalisation to hierarchical VAEs). See Fig 1 for a demonstration.

Thus our key contributions are:

- A demonstration that  $\beta$ -TCVAEs are significantly more robust to adversarial attacks via their latents than vanilla VAEs.
- The introduction of the *Seatbelt-VAE*, a hierarchical version of the  $\beta$ -TCVAE, designed both to increase the perceptual quality of reconstructions and to further increase robustness to various types of adversarial attack.

## 2 Background and Related Work

**VAEs** Variational autoencoders (VAEs) are a deep extension of factor analysis suitable for high-dimensional data like images [2, 3]. They have a joint distribution over data  $x$  and latent variables  $z$ :  $p_\theta(x, z) = p_\theta(x|z)p(z)$  where  $p(z) = \mathcal{N}(0, \mathcal{I})$  and  $p_\theta(x|z)$  is an appropriate distribution given the form of the data, the parameters of which are represented by deep nets with parameters  $\theta$ . As exact inference is intractable for this model, in a Variational Auto-encoder we perform amortised

stochastic variational inference. By introducing an approximate posterior distribution  $q_\phi(z|x) = \mathcal{N}(\mu_\phi(x), \Sigma_\phi(x))$ , we can perform gradient ascent on the evidence lower bound (ELBO)  $\mathcal{L}(x) = -\text{KL}_z(q_\phi(z|x)||p_\theta(x, z)) = \mathbb{E}_{q_\phi(z|x)} \log p_\theta(x|z) - \text{KL}(q_\phi(z|x)||p(z)) \geq \log p(x)$  w.r.t. both  $\theta$  and  $\phi$  jointly, using the reparameterisation trick to take gradients through Monte Carlo samples from  $q_\phi(z|x)$ .

**Disentangling VAEs** In a  $\beta$ -VAE [7], a free parameter  $\beta$  multiplies the KL term in  $\mathcal{L}(x)$  above. This objective  $\mathcal{L}_\beta(x)$  remains a lower bound on the evidence.

Decompositions of  $\mathcal{L}(x)$  shed light on its meaning. As shown in [20, 21, 4, 5, 6], one can define the evidence lower bound not per data-point, but instead write it over a dataset  $D$  of size  $N$ ,  $D = \{x^n\}$ , so we have  $\mathcal{L}(\theta, \phi, D)$ .

[6] gives a decomposition of this dataset-level evidence lower bound:

$$\begin{aligned} \mathcal{L}(\theta, \phi, D) &= -\text{KL}(q_\phi(z, x)||p_\theta(x, z)) & (1) \\ &= \mathbb{E}_{q_\phi(z, x)} \left[ \underbrace{\log \frac{p_\theta(x|z)}{p_\theta(x)}}_{\textcircled{1}} - \underbrace{\log \frac{q_\phi(z|x)}{q_\phi(z)}}_{\textcircled{2}} \right] - \underbrace{\text{KL}(q(x)||p_\theta(x))}_{\textcircled{3}} - \underbrace{\text{KL}(q_\phi(z)||p(z))}_{\textcircled{4}} & (2) \end{aligned}$$

where under the assumption that  $p(z)$  factorises we can further decompose  $\textcircled{3}$ :

$$\text{KL}(q_\phi(z)||p(z)) = \mathbb{E}_{q_\phi(z)} \left[ \underbrace{\log \frac{q_\phi(z)}{\prod_j q_\phi(z_j)}}_{\textcircled{A}} \right] + \sum_j \underbrace{\text{KL}(q_\phi(z_j)||p(z_j))}_{\textcircled{B}} & (3)$$

where  $j$  indexes over coordinates in  $z$ .  $q_\phi(z, x) = q_\phi(z|x)q(x)$  and  $q(x) := \frac{1}{N} \sum_{n=1}^N \delta(x - x^n)$  is the empirical data distribution.  $q_\phi(z) := \frac{1}{N} \sum_{n=1}^N q_\phi(z|x^n)$  is called the *average encoding distribution* following [20].

$\textcircled{A}$  is the total correlation (TC) for  $q_\phi(z)$ , a generalisation of mutual information to multiple variables [22]. With this mean-field  $p(z)$ , Factor and  $\beta$ -TCVAEs upweight this term, so we have an objective  $\mathcal{L}^{\beta TC}(\theta, \phi, D) = \textcircled{1} + \textcircled{2} + \textcircled{3} + \textcircled{B} + \beta \textcircled{A}$ . [5] gives a differentiable, stochastic approximation to  $\mathbb{E}_{q_\phi(z)} \log q_\phi(z)$ , rendering this decomposition simple to use as a training objective using stochastic gradient descent. We also note that  $\textcircled{A}$ , the total correlation, is also the objective in Independent Component Analysis (ICA) [23, 24].

**Hierarchical VAEs** We now have a set of  $L$  layers of  $z$  variables:  $\mathbf{z} = [z^1, z^2, \dots, z^L]$ . The evidence lower bound for models of this form is:

$$\mathcal{L}^{\text{DLGM}}(\theta, \phi, D) = \mathbb{E}_{q_\phi(\mathbf{z}, x)} \log \frac{p_\theta(x, \mathbf{z})}{q_\phi(\mathbf{z}, x)} = \mathbb{E}_{q_\phi(\mathbf{z}, x)} [\log p_\theta(x|\mathbf{z})] - \mathbb{E}_{q(x)} [\text{KL}(q_\phi(\mathbf{z}, x)||p_\theta(\mathbf{z}))] & (4)$$

The simplest VAE with a hierarchy of conditional stochastic variables in the generative model is the Deep Latent Gaussian Model [3]. The forward model factorises as a chain:

$$p_\theta(x, \mathbf{z}) = p_\theta(x|z^1) \prod_{i=1}^{L-1} p_\theta(z^i|z^{i+1}) p(z^L) & (5)$$

Each  $p_\theta(z^i|z^{i+1})$  is a Gaussian distribution with mean and variance parameterised by deep nets.  $p(z^L)$  is a unit isotropic Gaussian.

We can understand this additional expressive power as coming from having a richer family of distributions for the likelihood over data  $x$  marginalising out all intermediate layers:  $p_\theta(x|z^L) = \int \prod_{i=1}^{L-1} dz^i p_\theta(x, \mathbf{z})$  is a non-Gaussian, highly flexible, distribution.

To perform amortised variational inference one introduces a recognition network, which can be any directed acyclic graph where each node, each distribution over each  $z^i$ , is Gaussian conditioned on its parents. This could be a chain, as in [3]:

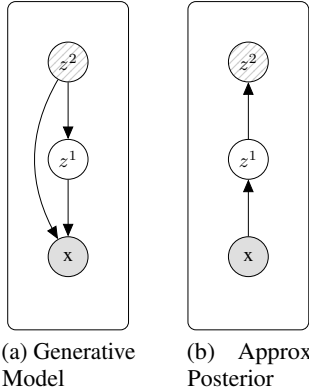
$$q_\phi(\mathbf{z}|x) = \prod_{i=1}^{L-1} q_\phi(z^{i+1}|z^i) q_\phi(z^1|x) & (6)$$

Again, marginalising out intermediate  $z^i$  layers, we see  $q_\phi(z^L|x) = \int \prod_{i=1}^{L-1} dz^i q_\phi(\mathbf{z}|x)$  is a non-Gaussian, highly flexible, distribution.

However, training DLGMs is challenging: the latent variables furthest from the data can fail to learn anything informative [18, 25]. Due to the factorisation of  $q_\phi(\mathbf{z}|x)$  and  $p_\theta(x, \mathbf{z})$  in a DLGM, it is possible for a single-layer VAE to train in isolation within a hierarchical model: each  $p_\theta(z^i|z^{i+1})$  distribution can become a fixed distribution not depending on  $z^{i+1}$  such that each KL divergence present in the objective between corresponding  $z^i$  layers can still be driven to a local minima. [25] gives a proof of this separation for the case where the model is perfectly trained, i.e.  $\text{KL}(q_\phi(z, x)||p_\theta(x, z)) = 0$ .

This is the hierarchical version of the collapse of  $z$  units in a single-layer VAE [26], but now the collapse is over entire layers  $z^i$ . It is part of the motivation for the Ladder VAE [18] and BIVA [19].

### 3 Seatbelt-VAE: Hierarchical $\beta$ -TCVAE with Skip Connections



We propose novel hierarchical disentangled VAEs where we aim to disentangle only in the top-most latent variables  $z^L$ . Following the Factor and  $\beta$ -TCVAEs we upweight the term of the form of (A) for  $z^L$ . Empirically we find models of this type are unable to converge when disentangling at the bottom most layer, or when disentangling at each layer. Intuitively, we want to capture high-level disentangled information at the top, but leave lower layers free to learn rich entangled representations. If  $p_\theta(x, \mathbf{z}) = p_\theta(x, z^1)$ , we obtain the generalisation of  $\beta$ TC penalisation to a DLGM, and we call it  $\beta$ -TCDLGM. It suffers from the problems of collapse described above.

Inspired by BIVA [19], instead we choose to condition our likelihood on all  $z^i$  layers:

Figure 2:  $L = 2$  Seatbelt-VAE. Shaded lines indicate  $\beta$ -TC factorisation in a given node.

$$p_\theta(x, \mathbf{z}) = p_\theta(x|\mathbf{z}) \prod_{i=1}^{L-1} p_\theta(z^i|z^{i+1})p(z^L) \quad (7)$$

Combining Eqs (6, 4, 7) and applying  $\beta$ -TC penalisation to the KL term over  $z^L$ :

$$\begin{aligned} \mathcal{L}^{\text{SB}}(\theta, \phi, D, \beta) &= \mathbb{E}_{q_\phi(\mathbf{z}, x)} \log p_\theta(x|\mathbf{z}) - \mathbb{E}_{q(x)} \log q(x) - \mathbb{E}_{q(x, z^2)} [\text{KL}(q_\phi(z^1|x)||p_\theta(z^1|z^2))] \\ &\quad - \sum_{m=2}^{L-1} \mathbb{E}_{q_\phi(z^{m-1}, z^{m+1})} [\text{KL}(q_\phi(z^m|z^{m-1})||p_\theta(z^m|z^{m+1}))] \\ &\quad - \text{KL}(q_\phi(z^L, z^{L-1})||q_\phi(z^L)q_\phi(z^{L-1})) - \beta \text{KL}(q_\phi(z^L)||\prod_{j=1} q_\phi(z_j^L)) \\ &\quad - \sum_j \text{KL}(q_\phi(z_j^L)||p(z_j^L)) \end{aligned} \quad (8)$$

where  $j$  is indexing over the coordinates in  $z^L$ . See Appendix for the derivation. We call this model *Seatbelt-VAE*, as with the extra conditional dependencies and nodes we increase the safety of our model: to adversarial attacks, to noise, and to decreases in perceptual quality as  $\beta$  increases. We find that using *free-bits* regularisation [27] greatly ameliorates the optimisation challenges associated with DLGMs. For  $L = 1$  this reduces to a  $\beta$ -TCVAE, and for  $L > 1, \beta = 1$  it produces a DLGM with our augmented likelihood function.

### 4 Robustness of VAEs to Adversarial Attacks

Most adversarial attack research has focused on discriminative models [28, 29] and recently VAEs have found use in protecting discriminative models against attack [30, 31]. Currently, two adversarial modes have been proposed for attacking VAEs [9, 10, 11]. In both attack modes the adversary wants

draws from the model  $x^{\text{rec}}$  to be close to a target image  $x^t$ , when given a distorted image  $x^* = x + d$  as input.

The first mode of attack, which we call the *output attack*, aims to reward draws from the decoder conditioned on  $z \sim q_\phi(z|x^*)$  that are close to  $x^t$  via the ELBO.

For a vanilla VAE, this attack’s adversarial objective is:

$$\Delta_{\text{output}}(x, d, x^t; \lambda) = \mathbb{E}_{q_\phi(z|x+d)}[\log(x^t|z)] - \text{KL}(q_\phi(z|x+d)||p(z)) + \lambda||d|| \quad (9)$$

The second mode of attack, the *latent attack*, aims to find  $x^* = x + d$  such that  $q_\phi(z|x^*) \approx q_\phi(z|x^t)$  under some similarity measure  $r(\cdot, \cdot)$ , which implicitly means that the likelihood  $p_\theta(x^t|z)$  is high when conditioned on draws from the posterior of the adversarial example. This attack is important if one is concerned with using the encoder network of a VAE as part of downstream task. For a single stochastic layer VAE, the latent-space adversarial objective is:

$$\Delta_{\text{latent}}(x, d, x^t; \lambda) = r(q_\phi(z|x+d), q_\phi(z|x)) + \lambda||d|| \quad (10)$$

Note that both modes of attack penalise the  $L_2$  norm of  $d$ , prioritising smaller distortions.

For [9, 10]  $r(\cdot, \cdot)$  is  $\text{KL}(q_\phi(z|x+d)||q_\phi(z|x))$  and for [11] it is the  $L_2$  distance  $||z_1 - z_2||_2$ ,  $z_1 \sim q_\phi(z|x+d)$ ,  $z_2 \sim q_\phi(z|x)$  between draws from the corresponding posteriors or  $||\mu_\phi(x) - \mu_\phi(x+d)||_2$  between their means. All three papers find that the latent attack mode is as or more effective than the output attack for single layer VAEs both under perceptual evaluation and various proposed metrics [9, 10, 11].

For latent attacks, the choice of which layers to attack depends on model architecture. For DLGMs and  $\beta$ -TCDLGMs the attacker only needs to match at the bottom latent layer, due to the chain factorisation in the posterior, Eq (6), and as  $p_\theta(x|z) = p_\theta(x|z^1)$ . See Appendix for plots showing how effective this attack is regardless of  $\beta$  and  $L$ . For Seatbelt-VAEs attackers must target all latent layers, as all are used in the likelihood over data.

$$\Delta_{\text{latent}}^{\text{DLGM}}(x, d, x^t; \lambda) = r(q_\phi(z^1|x+d), q_\phi(z^1|x)) + \lambda||d|| \quad (11)$$

$$\Delta_{\text{latent}}^{\text{SB}}(x, d, x^t; \lambda) = \sum_{i=1}^L r(q_\phi(z^i|x+d), q_\phi(z^i|x)) + \lambda||d|| \quad (12)$$

## 5 Experiments

We used the same encoder and decoder architectures as [5] for each dataset. For the details of neural network architectures and training, see Appendix and accompanying code.

**ELBO and Reconstruction Quality:  $\beta$ -TCVAEs to Seatbelt-VAEs** Fig 3 shows that the ELBO for  $\beta$ -TCVAE declines with  $\beta$  much more strongly than Seatbelt VAEs or  $\beta$ -TCDLGMs. We also show that increasing  $\beta$  reduces KL collapse: see Appendix for plots.

In Fig 4 we see the effect of depth and disentangling on reconstructions of CelebA. The bottom row, showing the reconstructions from a Seatbelt-VAE with  $L = 4$  and  $\beta = 1, 10$  clearly maintains facial identity better than those from a  $\beta$ -TCVAE in the middle row. Perhaps the effect is clearest for the 3<sup>rd</sup>, 4<sup>th</sup> and 7<sup>th</sup> columns, where many of the individuals’ finer facial features are lost by the  $\beta$ -TCVAE but maintained by the Seatbelt-VAE.

**Adversarial Attack** We apply attacks minimising each of  $\Delta_{\text{output}}$  and  $\Delta_{\text{latent}}$ , the latter using the KL formulation of [9, 10], on: vanilla VAEs,  $\beta$ -TCVAEs,  $\beta$ -TCDLGMs and Seatbelt-VAEs; trained on: Chairs [32], 3D faces [33], and CelebA [34]; for a range of  $\beta, L$  and  $\lambda$  values. We randomly sampled 10 input-target pairs for each dataset. As in [9, 10], for each pair of images used,  $\{\lambda\} = \{0\} \cup \{2^c\}$  where  $c$  takes 50 equally spaced values from -20 to 20. Thus each model undergoes 500 attacks for each attack mode. We used L-BFGS-B for gradient descent [35].

As our datasets do not have a clear classification task, metrics where one measures the effect on a classifier that uses draws from  $q_\phi(z|x)$  as input [11] are not relevant. Instead, we evaluate the effectiveness of the adversarial attacks on different models from the minimal values reached by the attack objectives  $\{\Delta_{\text{output}}, \Delta_{\text{latent}}\}$  and by visually appraising the adversarial input  $x^* = x + d$  and the adversarial reconstruction  $x^{\text{rec}}$ . Note that higher objective values indicate less effective attacks.

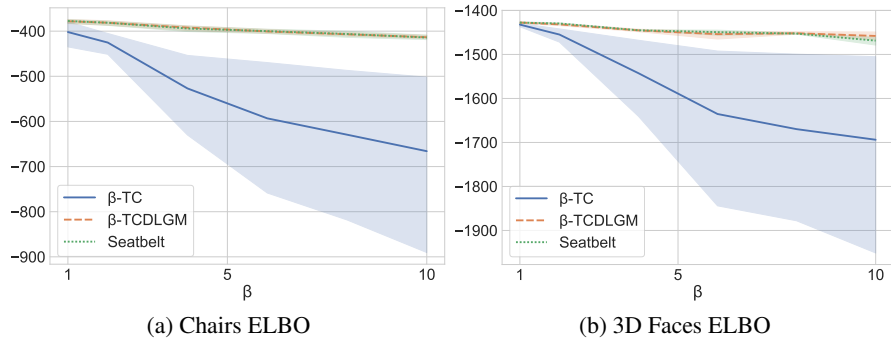


Figure 3: Plots showing the effect of varying  $\beta$  under various datasets on the ELBO of  $\beta$ -TCVAEs and Seatbelt-VAEs. Shading corresponds to the 95% CI over variation due to variation of  $\|z\|$  and  $L$  respectively.



Figure 4: Top row shows CelebA input data. Below are reconstructions from  $\beta$ -TCVAE,  $\beta = 20$  and then Seatbelt VAE,  $L = 4$ ,  $\beta = 20$ .

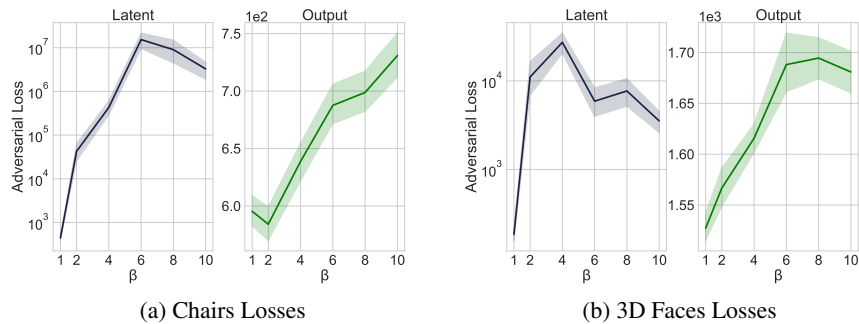


Figure 5:  $\Delta_{\text{latent/output}}$  for (a) Chairs (b) 3D Faces, for  $\beta$ -TCVAE for different  $\beta$  values. Shading corresponds to the 95% CI over variation due to our stable of images and our values of  $\|z\|$  and  $\lambda$ .

See Fig 1 for a demonstration of how latent adversarial attacks are made less effective in  $\beta$ -TC and Seatbelt-VAEs. In choosing which  $\lambda$  value to plot the attack for, we follow [10] and pick the largest  $\lambda$  which led to the smallest  $\Delta(x, d, x^t; \lambda)$  larger than  $1/50 \sum_{i=1}^{50} \Delta(x, d, x^t; \lambda(c_i))$ .

Fig 5 shows  $\beta$ -TCVAEs become harder to attack as  $\beta$  increases. The values of  $\Delta_{\text{latent}}$  for  $\beta$ -TCVAEs are  $\approx 10^3$  times higher than for a standard VAE on Chairs, and still greater than a factor of 10 for 3D faces. Attack via  $\Delta_{\text{output}}$  is also made less effective, but by a smaller factor  $\approx 1.2$ .

We find that  $\beta$ -TCDLGMs are easy to attack via output attacks and latent attacks - besides Fig 1 and Fig 6, see Appendix for detailed results and numerous examples. The latent space attack results substantiate our claim that an adversary only has to attack at the bottom-most latent layer.

We find that Seatbelt-VAEs are more robust still to latent and output attacks than  $\beta$ -TCVAEs. For high values of  $\beta$  and  $L$ , latent attacks often result in the outputs from adversarial attack looking very similar to the original input reconstruction (as visible in Fig 1 and in the Appendix). The output

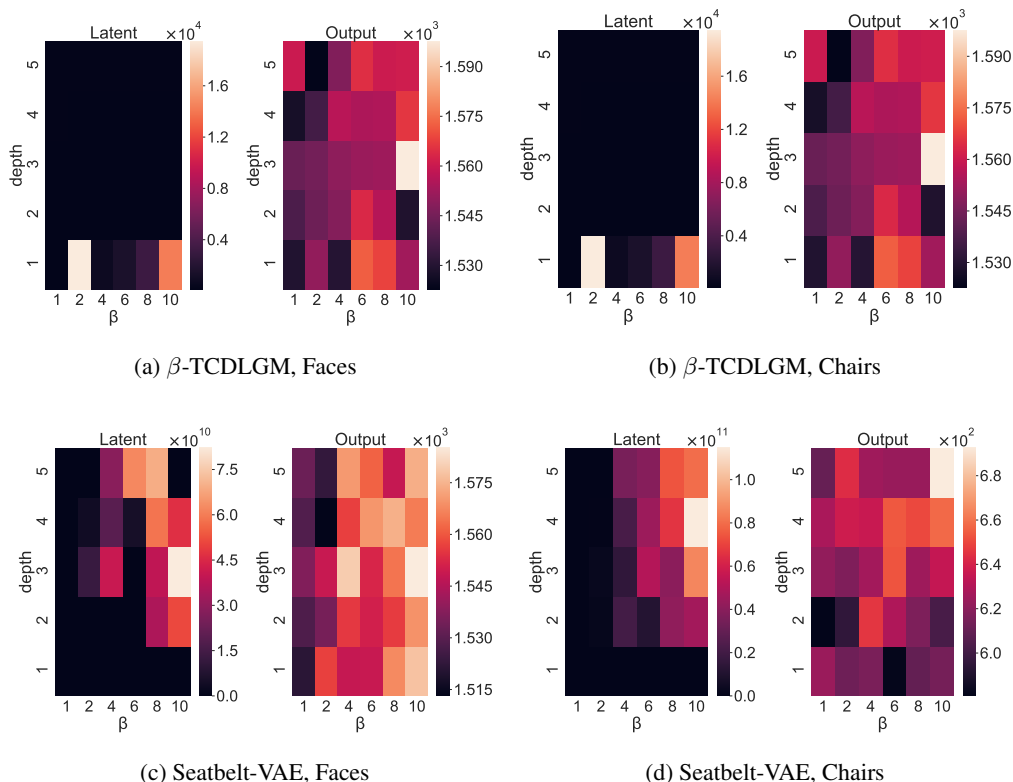


Figure 6:  $\{\Delta_{\text{latent}}, \Delta_{\text{output}}\}$  for (a) (b)  $\beta$ -TCDLGMs and (c) (d) Seatbelt-VAEs for Chairs and 3D Faces; over  $\beta$  and  $L$  values.

attack, which is less effective to begin with, is rendered less effective, but by a smaller margin. Note that we rarely observe perceptually effective output attacks regardless of model or settings.

Fig 6 shows the average adversarial objective for the two attack modes over a range of datasets for  $\beta$ -TCDLGMs and Seatbelt-VAEs. The  $\beta$ -TCDLGMs do not show higher latent attack objectives with  $L, \beta$ .

Like a  $\beta$ -TCVAE, Seatbelt-VAEs offer significantly increased protection to latent attacks, and somewhat increased protection to output attacks. For Seatbelt-VAEs the top right corner, corresponding to high  $\beta$ , large  $L$  models generally contains the largest values of adversarial objective.  $\Delta_{\text{latent}}$  grows by a factor of  $\approx 10^7$  from  $\beta = 1, L = 1$  to  $\beta = 10, L = 5$ , for each dataset.

The bottom row of Fig 6 (c) (d) have  $L = 1$ , so are  $\beta$ -TCVAEs. They contain relatively low values of the adversarial objectives compared to  $L > 1$ . Similarly the first column, corresponding to  $\beta=1$  models, contains relatively low values. This figure shows that depth and disentangling together offer the most effective protection from the two adversarial attacks studied over these datasets.

See Appendix for numerous examples of the attacks themselves under  $\{\Delta_{\text{latent}}, \Delta_{\text{output}}\}$  for: vanilla VAEs,  $\beta$ -TCVAEs,  $\beta$ -TCDLGMs and Seatbelt VAEs; over dSprites (a toy dataset for disentangling), Chairs, 3D Faces and CelebA; each over a range of  $\beta, L$ , and  $\lambda$ . There we also calculate the  $L_2$  distance between target images and adversarial outputs and show that the loss of effectiveness of adversarial attacks is not simply due to the degradation of reconstruction quality from increasing  $\beta$  penalties. By these metrics too Seatbelt-VAEs outperform both  $\beta$ -TCVAEs and VAEs.

**Robustness to Noise** All data fed to encoders in our models is scaled to  $-1 \leq x \leq 1$ . To test robustness to noise, we add  $\epsilon \sim \mathcal{N}(0, \mathcal{I})$  to the datasets and then evaluate  $\mathbb{E}_{q-\phi(z|x+\epsilon)} p_{\theta}(x|z)$  of the unnoised data. See Fig 7 for smoothed histogram plots of this for different models for different degrees of  $\beta$ . Both  $\beta$ -TC and Seatbelt-VAEs become more robust to noise with increasing  $\beta$ , while  $\beta$ -TCDLGMs get worse. The plots here partially explain why Seatbelt-VAEs can be unaffected

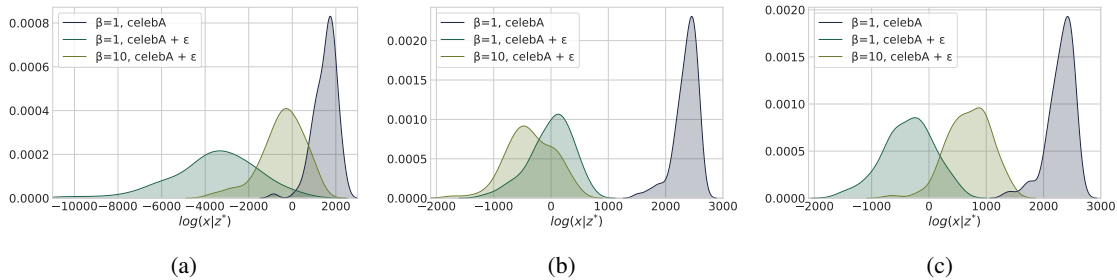


Figure 7: Robustness of  $\log p_{\theta}(x|z)$  to additive Gaussian noise  $\epsilon \sim \mathcal{N}(0, \mathcal{I})$  on  $x$  for CelebA under (a)  $\beta$ -TCVAE (b)  $\beta$ -TCDLGM,  $L = 4$  (c) Seatbelt VAE,  $L = 4$ ; for  $\beta = 1, 10$ . The x-axis for (a) is different to (b) and (c).

Table 1:  $L_2$  of Encoders and Decoders by dataset for  $\beta$ -TCVAE and Seatbelt-VAE ( $L = 4$ ) showing the proportional change from increasing  $\beta$  from 1 to 10.

		Chairs	3D Faces	CelebA
		$\beta : 1 \rightarrow 10$	$\beta : 1 \rightarrow 10$	$\beta : 1 \rightarrow 10$
Encoder	$\beta$ -TCVAE	+5.0%	+19.5%	+73.7%
	Seatbelt-VAE, $L = 4$	+1.0%	+2.7%	+40.2%
Decoder	$\beta$ -TCVAE	-19.4%	-15.0%	-6.8%
	Seatbelt-VAE, $L = 4$	-7.6%	-6.0%	-11.4%

by the distortions applied to the input during latent space attacks: they are effectively denoising autoencoders. See Appendix for plots showing the robustness of these models to smaller magnitude noise.

**Total Correlation Penalisation as Regularisation** In the auto-encoder view of these models, the KL terms in  $\mathcal{L}(\theta, \phi, D)$  are associated with a form of regularisation of the model [36]. Recent work shows that for linear autoencoders  $L_2$  regularisation of the weights corresponds to orthogonality of the latent projections [37]. For deep models we expect that disentangling is associated with simpler decoders and more complicated encoders. The decoder receives a simpler representation to work with, but building this representation requires more calculation. Here we measure the  $L_2$  norm of the weights of our networks as a function of  $\beta$ , shown in Table 1. See Appendix for results for  $\beta$ -TCDLGM.

As we increase  $\beta$  for  $\beta$ -TCVAEs and Seatbelt-VAEs for Chairs, 3D Faces, and CelebA the  $L_2$  norm increases for the encoder and decreases for the decoder. That the changes are generally greater for  $\beta$ -TCVAE than Seatbelt-VAE makes sense, as the encoder and decoder of the former interact directly with the disentangled representation. For the latter the encoder output is mapped through multiple MLPs before being disentangled in  $z^L$  and the decoder receives inputs from all  $z^t$ , of varying degrees of disentanglement.

## 6 Conclusion

We have presented the increases in robustness to adversarial attack afforded by  $\beta$ -TCVAEs. This increase in robustness is strongest for attacks via the latent space. While disentangled models are often motivated by their ability to provide interpretable conditional generation, many use cases for VAEs centre on the learnt latent representation of data. Given the use of these representations as inputs for other tasks, the latent attack mode is the most important to protect against. We introduce Seatbelt-VAE, a particular hierarchical VAE disentangled on the top-most layer with skip connections down to the decoder. This model further increases robustness to adversarial attacks, while also increasing the quality of reconstructions. The performance of our model under adversarial attack to robustness is mirrored in robustness to uncorrelated noise: these models are effective denoising autoencoders as well. We hope this work stimulates further interest in defending, and attacking, VAEs.

## References

- [1] Irina Higgins, David Amos, David Pfau, Sebastien Racaniere, Loic Matthey, Danilo Rezende, and Alexander Lerchner. Deepmind. Towards a Definition of Disentangled Representations. *CoRR*, 2018.
- [2] Diederik P Kingma and Max Welling. Auto-Encoding Variational Bayes. In *NeurIPS*, 2013.
- [3] Danilo Jimenez Rezende, Shakir Mohamed, and Daan Wierstra. Stochastic Backpropagation and Approximate Inference in Deep Generative Models. In *ICML*, 2014.
- [4] Hyunjik Kim and Andriy Mnih. Disentangling by Factorising. In *NeurIPS*, 2018.
- [5] Ricky T Q Chen, Xuechen Li, Roger Grosse, and David Duvenaud. Isolating Sources of Disentanglement in Variational Autoencoders. In *NeurIPS*, 2018.
- [6] Babak Esmaeili, Hao Wu, Sarthak Jain, Alican Bozkurt, N Siddharth, Brooks Paige, Dana H Brooks, Jennifer Dy, and Jan-Willem van de Meent. Structured Disentangled Representations. *CoRR*, 2018.
- [7] Irina Higgins, Loic Matthey, Arka Pal, Christopher Burgess, Xavier Glorot, Matthew Botvinick, Shakir Mohamed, and Alexander Lerchner.  $\beta$ -VAE: Learning Basic Visual Concepts with a Constrained Variational Framework. In *ICRL*, 2017.
- [8] Alexander A Alemi, Ian Fischer, Joshua V Dillon, and Kevin Murphy. Deep Variational Information Bottleneck. In *ICLR*, 2017.
- [9] Pedro Tabacof, Julia Tavares, and Eduardo Valle. Adversarial Images for Variational Autoencoders. In *NIPS Workshop on Adversarial Training*, 2016.
- [10] George Gondim-Ribeiro, Pedro Tabacof, and Eduardo Valle. Adversarial Attacks on Variational Autoencoders. *CoRR*, 2018.
- [11] J Kos, I Fischer, and D Song. Adversarial Examples for Generative Models. In *IEEE Security and Privacy Workshops*, pages 36–42, 5 2018.
- [12] Weidi Xu, Haoze Sun, Chao Deng, and Ying Tan. Variational Autoencoder for Semi-supervised Text Classification. In *AAAI*, pages 3358–3364, 2017.
- [13] Matt J Kusner, Brooks Paige, and José Miguel Hernández-Lobato. Grammar Variational Autoencoder. In *ICML*, 2017.
- [14] Lucas Theis, Wenzhe Shi, Andrew Cunningham, and Ferenc Huszár. Lossy Image Compression with Compressive Autoencoders. In *ICLR*, 2017.
- [15] James Townsend, Tom Bird, and David Barber. Practical Lossless Compression with Latent Variables using Bits Back Coding. *ICLR*, 2019.
- [16] David Ha and Jürgen Schmidhuber. World Models. In *NeurIPS*, 2018.
- [17] Irina Higgins, Arka Pal, Andrei Rusu, Loic Matthey, Christopher Burgess, Alexander Pritzel, Matthew Botvinick, Charles Blundell, and Alexander Lerchner. DARLA: Improving Zero-Shot Transfer in Reinforcement Learning. In *ICML*, 2017.
- [18] Casper Kaae Sønderby, Tapani Raiko, Lars Maaløe, Søren Kaae Sønderby, Ole Winther, and Olwi@dtu Dk. Ladder Variational Autoencoders. In *NeurIPS*, 2016.
- [19] Lars Maaløe, Marco Fraccaro, Valentin Liévin, and Ole Winther. BIVA: A Very Deep Hierarchy of Latent Variables for Generative Modeling. *CoRR*, 2019.
- [20] Matthew D Hoffman and Matthew J Johnson. ELBO surgery: yet another way to carve up the variational evidence lower bound. In *NeurIPS*, 2016.
- [21] Alireza Makhzani, Jonathon Shlens, Navdeep Jaitly, Ian Goodfellow, and Brendan Frey. Adversarial Autoencoders. In *ICLR*, 2016.
- [22] Satoshi Watanabe. Information Theoretical Analysis of Multivariate Correlation. *IBM Journal of Research and Development*, 4(1):66–82, 1960.
- [23] Anthony J Bell and Terrence J Sejnowski. An information-maximisation approach to blind separation and blind deconvolution. *Neural Computation*, 7(6):1004–1034, 1995.
- [24] S Roberts and R Everson. *Independent Component Analysis: Principles and Practice*. Cambridge University Press, 2001.

- [25] Shengjia Zhao, Jiaming Song, and Stefano Ermon. Learning Hierarchical Features from Generative Models. In *ICML*, 2017.
- [26] Yuri Burda, Roger Grosse, and Ruslan Salakhutdinov. Importance Weighted Autoencoders. In *ICLR*, 2016.
- [27] Diederik P Kingma, Tim Salimans, Rafal Jozefowicz, Xi Chen, Ilya Sutskever, and Max Welling. Improving Variational Inference with Inverse Autoregressive Flow. In *NeurIPS*, 2016.
- [28] Naveed Akhtar and Ajmal Mian. Threat of Adversarial Attacks on Deep Learning in Computer Vision: A Survey. *IEEE Access*, 6:14410–14430, 2018.
- [29] Justin Gilmer, Ryan P Adams, Ian Goodfellow, David Andersen, and George E Dahl. Motivating the Rules of the Game for Adversarial Example Research. *CoRR*, 2018.
- [30] Lukas Schott, Jonas Rauber, Matthias Bethge, and Wieland Brendel. Toward the First Adversarially Robust Neural Network Model on MNIST. In *ICLR*, 2019.
- [31] Partha Ghosh, Arpan Losalka, and Michael J Black. Resisting Adversarial Attacks Using Gaussian Mixture Variational Autoencoders. In *AAAI*, 2019.
- [32] Mathieu Aubry, Daniel Maturana, Alexei A Efros, Bryan C Russell, and Josef Sivic. Seeing 3D chairs: Exemplar part-based 2D-3D alignment using a large dataset of CAD models. In *Proceedings of the IEEE Computer Society Conference on Computer Vision and Pattern Recognition*, pages 3762–3769, 2014.
- [33] Pascal Paysan, Reinhard Knothe, Brian Amberg, Sami Romdhani, and Thomas Vetter. A 3D face model for pose and illumination invariant face recognition. In *6th IEEE International Conference on Advanced Video and Signal Based Surveillance, AVSS 2009*, pages 296–301, 2009.
- [34] Ziwei Liu, Ping Luo, Xiaogang Wang, and Xiaoou Tang. Deep Learning Face Attributes in the Wild. In *Proceedings of International Conference on Computer Vision (ICCV)*, 2015.
- [35] Richard H Byrd, Peihuang Lu, Jorge Nocedal, and Ciyou Zhu. A Limited Memory Algorithm for Bound Constrained Optimization. *SIAM J. Sci. Comput.*, 16(5):1190–1208, 9 1995.
- [36] Carl Doersch. Tutorial on Variational Autoencoders. Technical report, Carnegie Mellon University, 2016.
- [37] Daniel Kunin, Jonathan M Bloom, Aleksandrina Goeva, and Cotton Seed. Loss Landscapes of Regularized Linear Autoencoders. In *ICML*, 2019.
- [38] Diederik P Kingma and Jimmy Lei Ba. Adam: A Method for Stochastic Optimisation. In *ICLR*, 2015.
- [39] Tejas D Kulkarni, Will Whitney, Pushmeet Kohli, and Joshua B Tenenbaum. Deep Convolutional Inverse Graphics Network. In *NeurIPS*, 2015.